Clumpy galaxies seen in H : inflated observed clump properties due to limited spatial resolution and sensitivity

Tamburello, Valentina ; Rahmati, Alireza ; Mayer, Lucio ; Cava, Antonio ; Dessauges-Zavadsky, Miroslava ; Schaerer, Daniel

Abstract: High-resolution simulations of star-forming massive galactic discs have shown that clumps form with a characteristic baryonic mass in the range 107–108 M , with a small tail exceeding 109 M produced by clump–clump mergers. This is in contrast with the observed kpc-size clumps with masses up to 1010 M in high-redshift star-forming galaxies. In this paper, we show that the comparison between simulated and observed star-forming clumps is hindered by limited observational spatial resolution and sensitivity. We post-process high-resolution hydrodynamical simulations of clumpy discs using accurate radiative transfer to model the effect of ionizing radiation from young stars and to compute H emission maps. By comparing the intrinsic clump size and mass distributions with those inferred from convolving the H maps with different Gaussian apertures, we mimic the typical resolution used in observations. We found that with 100 pc resolution, mock observations can recover the intrinsic clump radii and stellar masses, in agreement with those found by lensing observations. Instead, using a 1 kpc resolution smears out individual clumps, resulting in their apparent merging. This causes significant overestimations of the clump radii and therefore masses derived using methods that use their observed sizes. We show that limited sensitivity can also force observations to significantly overestimate the clump masses. We conclude that a significant fraction of giant clumps detected in the observations may result from artificially inflated radii and masses, and that 100 pc spatial resolution is required to capture correctly the physical characteristics of star-forming clumps if they are coherent structures produced by disc fragmentation.

DOI: https://doi.org/10.1093/mnras/stx784

Monthly Notices of the ROYAL ASTRONOMICAL SOCIETY

MNRAS **468,** 4792–4800 (2017) doi:10.1093/mnras/stx784
Advance Access publication 2017 March 30

Clumpy galaxies seen in H α: inflated observed clump properties due to limited spatial resolution and sensitivity

Valentina Tamburello,[1,2]★ Alireza Rahmati,[1] Lucio Mayer,[1,2] Antonio Cava,[3] Miroslava Dessauges-Zavadsky[3] and Daniel Schaerer[3,4]

[1]*Center for Theoretical Astrophysics and Cosmology, Institute for Computational Science, University of Zurich, Winterthurerstrasse 190, CH-8057 Zürich, Switzerland*
[2]*Physik-Institut, University of Zurich, Winterthurerstrasse 190, CH-8057 Zürich, Switzerland*
[3]*Observatoire de Genève, Université de Genève, 51 Ch. des Maillettes, CH-1290 Versoix, Switzerland*
[4]*CNRS, IRAP, 14 Avenue E. Belin, 31400 Toulouse, France*

Accepted 2017 March 28. Received 2017 March 28; in original form 2016 October 7

ABSTRACT

High-resolution simulations of star-forming massive galactic discs have shown that clumps form with a characteristic baryonic mass in the range 10^7–10^8 $M_\odot$, with a small tail exceeding 10^9 $M_\odot$ produced by clump–clump mergers. This is in contrast with the observed kpc-size clumps with masses up to 10^{10} $M_\odot$ in high-redshift star-forming galaxies. In this paper, we show that the comparison between simulated and observed star-forming clumps is hindered by limited observational spatial resolution and sensitivity. We post-process high-resolution hydrodynamical simulations of clumpy discs using accurate radiative transfer to model the effect of ionizing radiation from young stars and to compute H α emission maps. By comparing the intrinsic clump size and mass distributions with those inferred from convolving the H α maps with different Gaussian apertures, we mimic the typical resolution used in observations. We found that with 100 pc resolution, mock observations can recover the intrinsic clump radii and stellar masses, in agreement with those found by lensing observations. Instead, using a 1 kpc resolution smears out individual clumps, resulting in their apparent merging. This causes significant overestimations of the clump radii and therefore masses derived using methods that use their observed sizes. We show that limited sensitivity can also force observations to significantly overestimate the clump masses. We conclude that a significant fraction of giant clumps detected in the observations may result from artificially inflated radii and masses, and that ≈100 pc spatial resolution is required to capture correctly the physical characteristics of star-forming clumps if they are coherent structures produced by disc fragmentation.

Key words: galaxies: evolution – galaxies: formation – galaxies: high-redshift.

1 INTRODUCTION

Galaxies in the redshift range 1–3 appear different from their counterparts in the Local Universe. They have higher velocity dispersions, lower rotation to dispersion ratios and higher gas fractions. One of the most significant peculiarities of high-z galaxies is that they show irregular morphologies in their stellar component which are commonly referred to as 'clumps' (Elmegreen et al. 2005). These regions are also characterized by high star formation rates and can have sizes up to 1 kpc and masses higher than 10^9 $M_\odot$, which is much larger than the largest star-forming complexes known at low redshifts, such as Giant Molecular Clouds (GMCs). As they appear to be sites of enhanced star formation, clumpy structures are also identified in H α observations of high redshift galaxies (Genzel et al. 2011; Swinbank et al. 2012; Wisnioski et al. 2012; Livermore et al. 2012, 2015). The prevailing explanation for the existence of such oversized star-forming complexes at high redshift is that they are physically coherent objects, resulting from the fragmentation of massive gas-rich galactic discs induced by gravitational instability (Bournaud et al. 2010; Ceverino, Dekel & Bournaud 2010), although substructure might be present at a smaller scale (Bournaud 2016). This is based on the evidence that galactic discs at high redshift are indeed massive and considerably more gas-rich than at low redshift (Tacconi et al. 2010), implying that their characteristic scale of fragmentation as given by the Toomre instability theory should also be larger than at low redshift, where GMCs-sized objects are instead produced (Dekel & Krumholz 2013). Yet observations become increasingly more difficult at higher redshifts, since

★ E-mail: vtambure@physik.uzh.ch

galaxies become intrinsically smaller and their surface brightness decreases with redshift as $(1+z)^{-4}$. As a result only central bright regions of galaxies or extreme star-forming galaxies can be studied observationally. *HST* (*Hubble Space Telescope*) imaging of 0.15 arcsec allows to reach a resolution of 1–1.5 kpc at $z = 1$–2, while ground-based telescopes, even with adaptive optics where a resolution of 0.25 arcsec is achieved, have a resolution of ∼2.1 kpc at $z = 1.5$. These resolutions are very close to the typical observationally measured clump sizes. The fact that observed clump sizes are close to the resolution limits of typical observations is potentially worrisome in light of the prevailing theoretical interpretation based on a fragmentation scale as such sizes could be overestimated. Indeed, recent observations using gravitational lensing technique which allows us to reach much higher spatial resolutions (∼100 pc) found that clumps in lensed galaxies are much smaller (Jones et al. 2010; Adamo et al. 2013; Livermore et al. 2012, 2015). However, it should be noted that the galaxies probed using the lensing technique are typically at $z \sim 1$ and are less massive than the other studied clumpy galaxies which are at higher redshifts.

A question arises spontaneously: are also the intrinsic sizes of clumps in the massive discs at $z \sim 2$ smaller than usually claimed? Are their estimated masses correct or are they also affected by resolution limitations? In a recent study, Behrendt, Burkert & Schartmann (2016) used one of the highest resolution simulations of massive clumpy gas discs and found no giant clumps. Instead, they found clump-like structures produced by gravitational instability with typical initial masses of the order a few times 10^7 $M_\odot$. Mimicking observations and the resolution of the instruments, they showed that their small clumps (radius ∼35 pc) are distributed in loosely bound clusters and thus can appear as giant kpc-clumps since small-scale substructure would not be detectable in observations due to beam smearing. Remarkably, the kinematics of the clusters of clumps they obtained are in quite good agreement with observations of individual giant clumps in the $z \sim 2$ galaxies of Genzel et al. (2011). A caveat of these simulations is that they lack a stellar disc component and do not include star formation and feedback, which can affect fragmentation significantly (Moody et al. 2014; Tamburello et al. 2015; Oklopcic et al. 2017; Mandelker et al. 2017; Mayer et al. 2016). However, the characteristic mass scale of individual clumps that they found is comparable to that seen in lower resolution simulations of clumpy disc that include a stellar disc and a rich inventory of sub-grid physical processes (Tamburello et al. 2015) as star formation and stellar feedback. Moreover, in a companion letter (Dessauges-Zavadsky et al. 2017), we examine the effects of sensitivity and spatial resolution on the measured stellar masses comparing clumps selected in different ways and observed in strongly lensed galaxies or bank field galaxies limited by kpc resolutions. We find that together the two effects imply that the inferred very large clump stellar masses are most likely overestimated although at present these effects cannot be quantified observationally.

In this paper, we use selected simulations from Tamburello et al. (2015) to test if observed giant clumps could be the result of blending of smaller structures owing to insufficient resolution and/or sensitivity in the observations. The simulations we use include star formation and stellar feedback which is an improvement compared to previous studies that neglected these phenomena. Moreover, we post-process our simulations with detailed radiative transfer (RT) calculation to predict the expected Hα emission from the simulations. To perform a fair comparison with observations, we add noise/error to the mock Hα intensity maps and convolve them with Gaussian filters mimicking the PSF specifications of instruments and observations employed in the literature for studying clumpy galaxies.

This paper is organized as follows: Section 2 describes the initial conditions and design of the simulations, Section 3 includes the results and Section 4 summarizes the paper with our conclusions.

2 METHODS

2.1 Hydrodynamical simulations

In this paper, we focus on mocks of high-resolution hydrodynamical non-cosmological simulations of clumpy high-z gas-rich discs already presented in Tamburello et al. (2015). The detailed structural properties of all galaxy models are described in Table 2 of Tamburello et al. (2015). From the Tamburello et al. (2015) sample, we chose the simulation that undergoes more fragmentation and gives rise to the largest clumps while including the effect of feedback. This simulation has the initial stellar mass of 4×10^{10} $M_\odot$, embedded in a halo of 2.5×10^{12} $M_\odot$, making the galaxy models consistent with the stellar mass–halo mass relation predicted using abundance matching and other observational constraints (Behroozi, Wechsler & Conroy 2013).

The initial gas fraction is 0.5 and the spatial resolution (the gravitational softening length) is 100 pc. The simulation is performed with the N-body + smoothed particle hydrodynamic (SPH) code GASOLINE. In order to form a star, a gas particle has to have temperature lower than 3×10^4 K and density higher than 10 cm^{-3}. The star formation efficiency parameter is $\epsilon_{\rm SF} = 0.01$ and 4×10^{50} erg thermal energy is released into the ISM per supernovae event, shutting off the cooling of the neighbouring gas particles for a few 10s of Myr (see Stinson et al. 2006 and Tamburello et al. 2015). This galaxy results in a highly clumpy structure (approximately after 100 Myr) and resembles $z \sim 2$ star-forming galaxies. A key aspect for our purpose is that this simulation produced clumps that are smaller and less massive compared to most previous work on massive disc fragmentation, having radii ∼100–300 pc and masses in the range 10^7–10^8 $M_\odot$, with some rare exceptions that can reach up to 10^9 $M_\odot$ (Tamburello et al. 2015).

As will be explained in the next section, to produce Hα maps, we post-process them by performing RT simulations to accurately calculate the gas ionization state.

2.2 Radiative transfer and mock Hα maps

Our simulation is post-processed with the RT code TRAPHIC (Pawlik & Schaye 2008, 2011) to account for ionizing radiation from young stars and the meta-galactic ionizing radiation. For the background radiation we adopt a hydrogen photoionization rate of 10^{-12} s^{-1}, which is appropriate for redshift $z \sim 1$–3.[1] The effect of UVB on ionization is accounted for by a density-dependent self-shielding correction following Rahmati et al. (2013a). For stellar radiation, we assume all stellar particles younger than 5 Myr are contributing to hydrogen ionizing radiation all with identical photon production rates of 6×10^{46} photons s^{-1} $M_\odot^{-1}$. In other words, we neglect the metallicity dependence and precise age dependence of stellar emissivities. The choice for stellar ionizing emissivities is motivated by results from STARBURST99 (Leitherer et al. 1999) and varies by a factor of a few around our choice depending on assumed metallicity

[1] Notice that also changing this number up to 10 times lower values, appropriate for higher and lower redshifts, does not change the results.

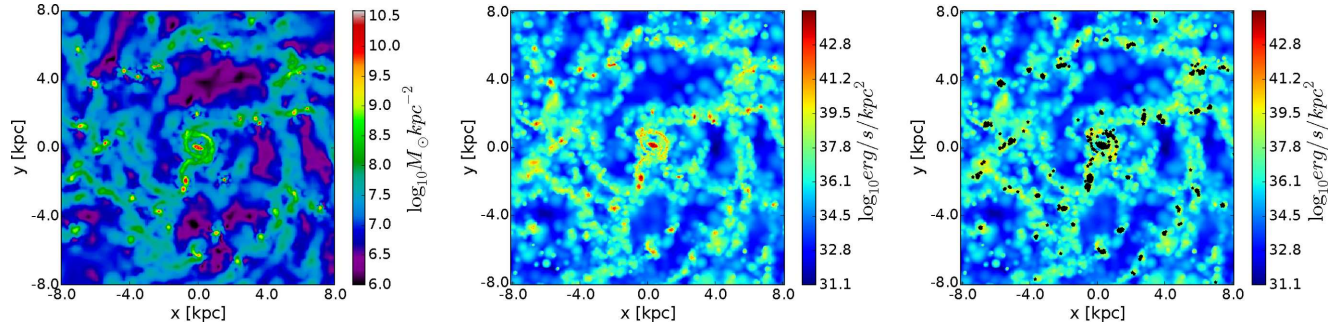

Figure 1. From left to right: gas density map, H α luminosity map obtained by post-processing simulation with radiative transfer and H α luminosity map with young stars (age <5 Myr, black stars). All the results are for a clumpy galaxy simulation at 200 Myr after the beginning of the simulation. H α clumps with sizes ∼100 pc are already present and closely trace star-forming regions.

and/or IMF (Rahmati et al. 2013b). For the energy distribution of ionizing radiation, we assume a blackbody radiation with an effective temperature of 4×10^4 K and we used Case-B recombination coefficient appropriate for the dense ISM gas. Then, sources can emit ionizing radiation and the RT code TRAPHIC follows the propagation of ionizing radiation in photon packets which travel with the speed of light and the ionization state of gas in post-processing (i.e. the distribution of gas and sources are fixed during the RT simulation). Then the RT simulation proceeds until the ionization equilibrium is reached. Collisional ionization is also accounted for.

After calculating the ionization state of the gas, we used SPH interpolation to make 2D H α maps of the simulated galaxy. In order to have the same resolution we have in Tamburello et al. (2015, ∼10 pc SPH smoothing length), we fixed the cell size at 10 pc. We calculate the intensity of H α emission for each pixel using:

$$I_\nu(\mathrm{H}\,\alpha) = \frac{h\nu(\mathrm{H}\,\alpha)}{4\pi} \int n_e n_p \alpha(\mathrm{H}\,\alpha) \mathrm{d}s, \quad (1)$$

where the integration is performed along the line of sight (ds, projection direction). For the temperature-dependent H α emission coefficient, we use $\alpha(\mathrm{H}\,\alpha) = 7.86 \times 10^{-14} \times 10^4 / T\,\mathrm{cm}^3\,\mathrm{s}^{-1}$, following Osterbrock & Ferland (2006). We note that normalizing the total luminosity of our mock maps with the star formation rate of the galaxy, using the following relation from Kennicutt (1998)

$$\mathrm{SFR}(\mathrm{M}_\odot \mathrm{yr}^{-1}) = \frac{\mathrm{L}(\mathrm{H}\,\alpha)}{1.26 \times 10^{41} \mathrm{ergss}^{-1}} \quad (2)$$

produces results which do not change our conclusions.[2] We do not include dust extinction, whose precise modelling is beyond the scope of this work.

2.3 Identifying the clumps

After producing the H α maps, in order to mimic observations, we add errors equivalent to 1 per cent, 5 per cent and 10 per cent of the total H α luminosity, uniformly distributed among all pixels (e.g. in the case of 1 per cent error, we added to each pixel an error of 0.01 × total luminosity of the map divided by the total number of pixels). We note that the values we chose bracket the typical observational errors one finds in the literature, encompassing all sources of error (e.g. noise, dust extinction modelling). We accept as signal everything that is above $5 \times n$, where n is the error per pixel, in order to be consistent with observations (sometimes a threshold of $3 \times n$ is used, but we check that our results are not affected by this change). The background (every signal lower than $5 \times n$) is set to zero for simplicity. Finally, in order to mimic the instrumental resolution effects, we convolve the H α maps with a 2D Gaussian aperture with different values of FWHM: 100 pc, appropriate for comparison with clumps found in lensed galaxies and 1 kpc, which is comparable to the typical resolution accessible for *HST* observations at $z \geq 1$. To identify the clumps in our H α luminosity maps, we proceed iteratively as follows. First of all, we find the maximum point of luminosity, $P_{\max} = (x_{\max}, y_{\max})$, in the map, then, by means of circles of increasing radius, R_i, in steps indexed by i around $P_{\max}$, we analyse the integrated luminosity associated with the clump candidate, that is

$$L_i(R_i) = \int_0^{R_i} l(r)\mathrm{d}r \quad (3)$$

We set the clump radius R_{clump} when either an area of background (set to zero) is reached, i.e. $l(R_{\mathrm{clump}}) = 0$, or when the average radial luminosity density, defined as

$$\int_{R_{i-1}}^{R_{\mathrm{clump}}} l(r)\mathrm{d}r / (R^2_{\mathrm{clump}} - R^2_{i-1}) \quad (4)$$

is increasing, most likely related to the presence of another clump. Once a clump is found, it is removed from the map and we return to the first step. To prevent the possibility of having spurious clumps, we consider in our analysis only clumps which have radii 10 times the cell size, so that the minimum clump radius is 100 pc. Moreover, for our analysis, we only consider clumps which have sizes equal to or larger than the Gaussian aperture used for smoothing the maps (e.g. radius of 500 pc for the smoothing using FWHM = 1 kpc).

3 RESULTS

Here we present our main results to investigate the effect that resolution has in determining the observed clump sizes and masses, and how these compare with the intrinsic clump sizes and masses in the simulations. The left-hand diagram in Fig. 1 shows the simulated gas density map at 200 Myr. The middle panel shows H α

[2] We note that Kennicutt (1998) assumed a Salpeter IMF for their calculations while we use a Krupa IMF in our simulations. The difference caused by the IMF choice is an offset in the normalization of the H α maps with a magnitude comparable to or smaller than the uncertainty involved in our simplified source modelling. Moreover, changing the normalization of our H α maps does not change the resulting clump properties and how they vary depending on resolution/sensitivity. However, we take the difference into account when comparing the SFR of the simulated clumps with observations (see Fig. 7).

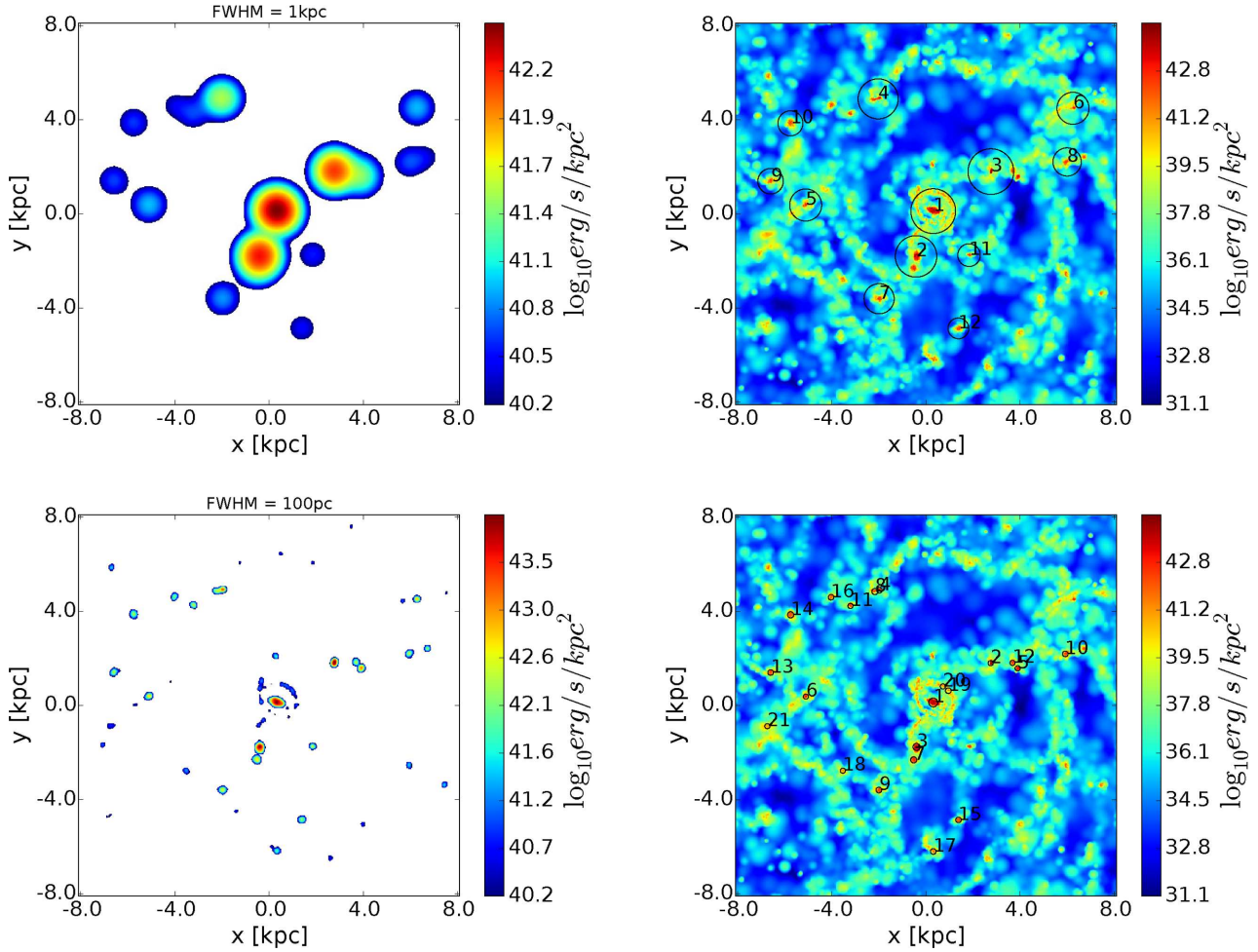

Figure 2. The left column shows identified clumps in the simulated α luminosity maps for the clumpy run at 200 Myr using 1 kpc (top) and 100 pc (bottom) smoothing length and an error level of 10 per cent (after subtracting the background). On the right column, the original simulated H α luminosity maps are shown with identified clumps in the convolved maps overplotted using circles. Lowering the spatial resolution makes the clumps appear larger.

map, while the right-hand panel shows the same with the position of young stars (the main ionizing sources in our calculations) overplotted using black dots. Comparing these two images, one can see that gas clumps are star-forming regions, well tracked by H α. Therefore, while H α is a tracer of ionized gas, it also performs well as a tracer of star-forming regions (young stars). In Fig. 2, we show how the H α luminosity map appears once we convolve it with a 2D Gaussian aperture with FWHM = 1 kpc (top left panel) and FWHM = 100 pc (bottom left panel). To show the sensitivity of H α clump properties to the underlying spatial resolution, in each map in Fig. 2, we also show the identified clumps with black circles.[3] When clumps are selected in the convolved map with FWHM = 1 kpc, indeed, they appear larger, because either they merge together or flux is smeared out. However, identified clumps in the map with FWHM = 100 pc are well resolved, nearly as good as they are in the original simulated maps without any smoothing. Moreover, the number of clumps in the higher resolution map is nearly twice the number of clumps identified in the lower resolution map. We repeat this analysis at different times (200, 300, 400 and 500 Myr), using different error values and convolution lengths. At each time we compute the H α clump radii and masses. Combining all the time steps, the distribution of H α clump radii is shown in the top row of Fig. 3. We show the results for both the resolutions obtained using FWHM = 100 pc (on the left-hand side) and FWHM = 1 kpc (on the right-hand side). Clumps selected after a Gaussian convolution with FWHM = 100 pc have sizes ∼100 pc as we previously showed in Tamburello et al. (2015), but their sizes increase up to 1 kpc when we make use of the Gaussian convolution with FWHM = 1 kpc. The result is not too sensitive to the level of error, however, the larger the error is, the fewer clumps we are able to find.

The clump gas mass distributions using FWHM = 100 pc (on the left-hand side) and FWHM = 1 kpc (on the right-hand side) and different errors are shown in the second row of Fig. 3. Here we define the clump mass as the total (neutral and ionized) gas within the clump radius, using a 2D gas density map. We also measure the stellar mass for each clump in the same way, by measuring the total stellar mass within an aperture defined by the clump radius in H α maps. This is very similar to the method used by Förster Schreiber et al. (2011) to identify stellar clumps and to calculate their masses using H_{160} band observations. However, we should stress that we identify our clumps using H α, which probes gas

[3] Note that in both cases our biggest clump, which is the most massive one too, is near the centre of the galaxy and corresponds to the bulge, which we found to be a generic result in our simulations.

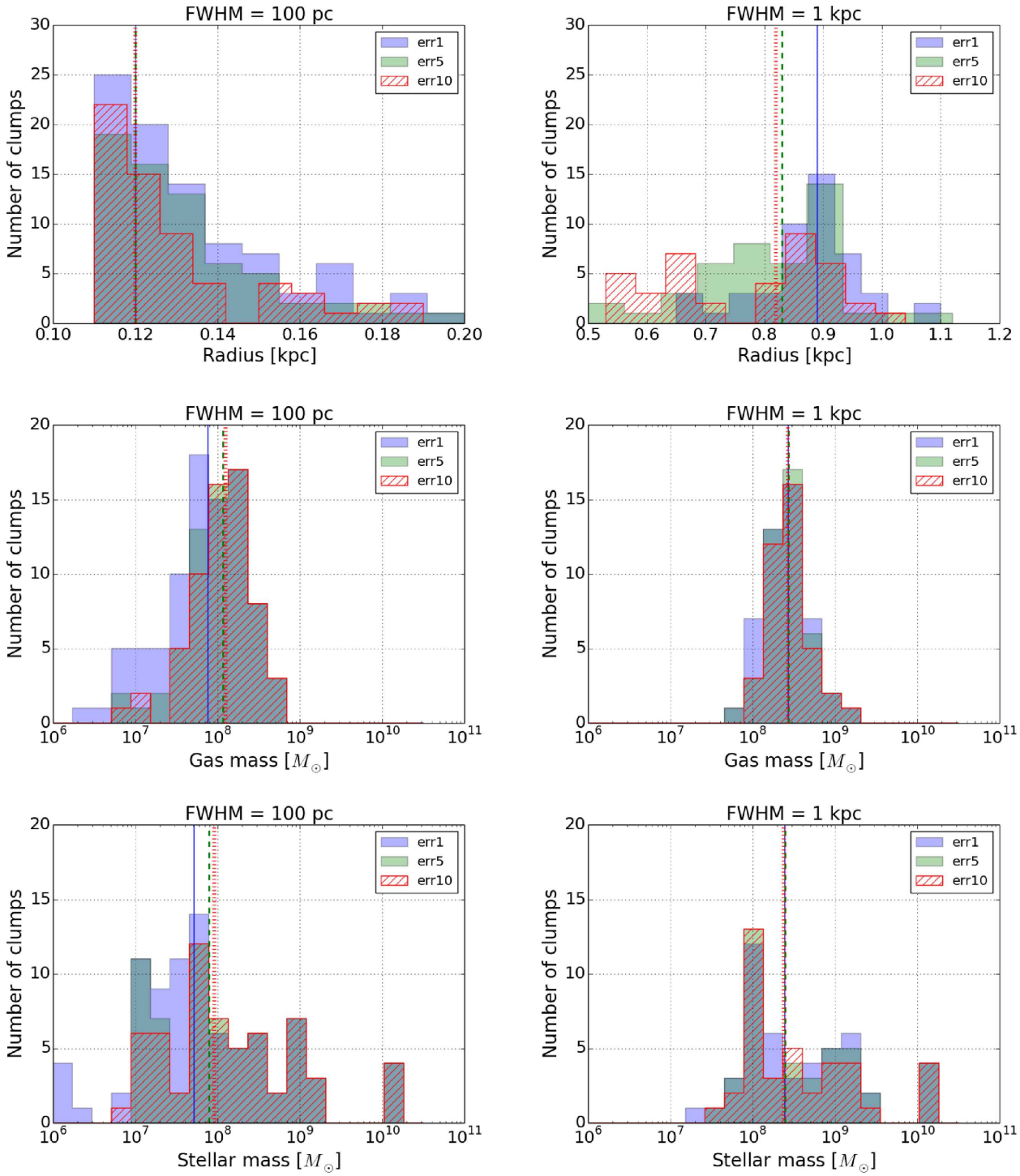

Figure 3. From top to bottom we show the Hα clump radius, total gas (neutral and ionized) mass and stellar mass distributions for our simulation combining different times (200, 300, 400 and 500 Myr) and using different levels of error (i.e. 1 per cent, 5 per cent and 10 per cent of the total luminosity). Distributions are obtained based on Hα maps convolved with FWHM = 100 pc (left) and FWHM = 1 kpc (right), using different levels of error. The medians of the distributions for the error levels of 1 per cent, 5 per cent and 10 per cent are shown using solid, dashed and dotted vertical lines, respectively. The results are weakly sensitive to the level of error. The clump sizes strongly vary by changing the observed spatial resolution, while clumps masses (both stellar and gaseous) are less sensitive to it.

properties and is not directly comparable with clumps identified in the stellar component. We find fewer, but more massive (by a factor of $\sim$2) clumps with FWHM = 1 kpc, compared to the case with FWHM = 100 pc for both gas and stellar mass estimates. The peak of both gas and stellar mass distributions for the lower resolution case is at $\sim 2 \times 10^8$ M$_\odot$. The sensitivity of the mass distributions to the spatial resolution is not as strong as that for the clump radius distribution. While the typical clump radius becomes 10 times larger by changing the spatial resolution from FWHM = 100 pc to FWHM = 1 kpc, the typical clump mass changes only by a factor

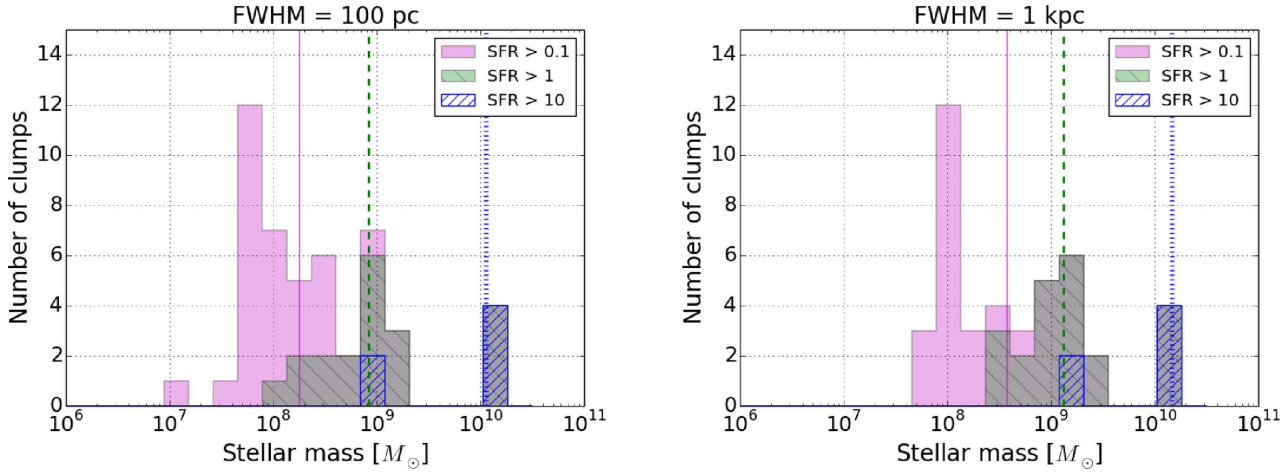

Figure 4. The sensitivity of stellar mass distribution of H α clumps to the detection threshold used for observing them. The mass distributions are shown for H α maps with 5 per cent error levels and for two different spatial resolution (100 pc on the left and 1 kpc on the right) and after combining different times (200, 300, 400 and 500 Myr). For each resolution the mass distributions are shown for SFR thresholds of 0.1, 1 and 10 $M_\odot$/yr and the vertical solid, dashed and dotted lines show their corresponding medians. The detection threshold (sensitivity) strongly affects the mass distribution of the clumps irrespective of the spatial resolution.

of 2. This is due to the fact that the convolution simply spreads out the same amount of mass/luminosity over a much larger area which strongly affects their measurable sizes. However, since most of the mass in the larger area is still inside the intrinsic radius of the clumps, the effect on the measured masses is not expected to be large. None the less, when two massive clumps are relatively close, as it is often the case since clump–clump mergers are common, the larger area would encompass the sum of their mass, which explains the factor of $\sim$2 increase in the mass distribution of the clumps as we decrease the spatial resolution. Finally, we note that our most massive clumps ($\sim 10^{10}$ $M_\odot$) correspond to the centre of our simulated galaxy, the bulge. We decide to include these bulge clumps in our analysis because observations usually cannot distinguish between bulge and clumps at high redshift, therefore the average clump mass can be overestimated also by the bulge existence.

The observed masses of the clumps could be more affected by another feature of the observations, namely their sensitivity limit. At any given sensitivity only objects brighter than the corresponding detection threshold are observed. Fig. 4 shows how using three different detection thresholds (SFR $>$ 0.1, 1, 10 $M_\odot$ yr^{-1}) results in drastically different clump stellar mass distributions, irrespective of the used spatial resolution.[4] Changing the sensitivity within the aforementioned range by a factor of 10 translates into nearly one order of magnitude change in the typical clump stellar mass. For a fixed detection threshold, however, changing the resolution from 100 pc to 1 kpc modifies the typical clump stellar mass by a factor of $\lesssim 2$. This is in nice agreement with what we find in Dessauges-Zavadsky et al. (2017), when comparing the observed clump stellar masses. The sensitivity effect appears more important than the spatial resolution effect, the former leading to a difference of more than an order of magnitude in stellar mass distributions of clumps in the lensed galaxies and in the field galaxies with a shallow clump selection, and the latter yielding a difference of roughly a factor of 4 in stellar mass distributions of clumps in the lensed galaxies and in the field galaxies with a deep clump selection.

Moreover, it is important to recall that, unlike simulations, observations do not have direct access to the actual mass inside the clumps and indirect methods should be used to estimate the observed clump masses (e.g. Genzel et al. 2011). Such methods often are based on specific theoretical assumptions about the nature of the clumps, such as assuming that clumps are bound and/or virialized objects. In these cases the measured masses would be significantly inflated simply because they are derived using equations that express the mass as a function of the observed radius, which, as we have shown, can be overestimated by an order of magnitude. For illustration, we can adopt the notion that clumps are virialized. In this case the clump mass, M, radius, R and velocity, v, are connected by the relation $M = v^2R/G$, where G is the gravitational constant. The velocity estimates are often based on high-resolution spectra and they are less prone to uncertainties related to the limited spatial resolution (see also Ceverino et al. 2012); so, in order to be conservative, we will assume they can be estimated correctly. Our clumps, having radii of $\sim$100 pc, could be seen as kpc-size objects (see the first row in Fig. 3), which leads to their masses being overestimated by one order of magnitude. As a result, a typical clump in the mass range of $\approx 10^8$ $M_\odot$ and the radius range of $\sim$120 pc would be seen as a kpc-size clump with an overestimated mass of $\sim 2 \times 10^9$ $M_\odot$, while directly measuring the mass inside the new aperture (size of the clump using low resolution) results in $\approx 3 \times 10^8$ $M_\odot$. Some published works have also assumed that the observed clump radius is proportional to the Jeans length λ_J (Wisnioski et al. 2012), which would imply that its mass is of order of the Jeans mass $M_J = (\lambda_J/2)^3 \times \rho_g$, where ρ_g is the mean local gas density in the disc. This results in the clump mass to scale as $\lambda_J^3/2^3 \sim (\lambda_J)^3/8$. With the latter scaling, even if the radius is overestimated by only a factor of 2, the corresponding mass will be overestimated by about an order of magnitude.

There are observational constraints on the sizes and masses of stellar clumps detected in high redshift galaxies (e.g. Förster Schreiber et al. 2011) that in principle could be used to compare with our simulations. Note, however, that there is a fundamental difference between clumps detected in the stellar component of a

[4] We note that the sensitivity thresholds we chose bracket the typical sensitivities accessible for current observations. For instance, to detect H α emission equivalent to SFR $\approx$0.1 with VLT and at $z \sim 3$ one needs more than $\approx$10 h of integration time.

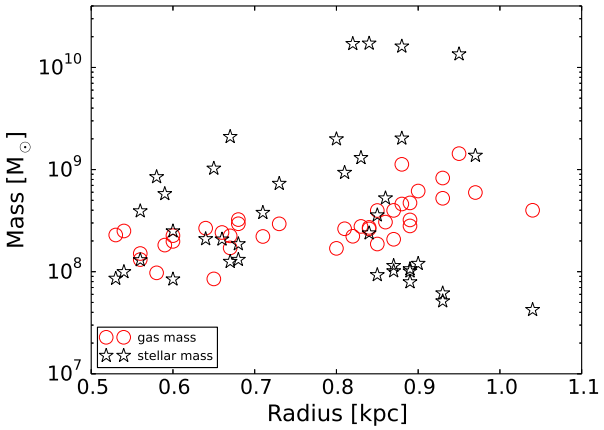

Figure 5. The simulated clump gas/stellar mass versus radius relation (shown with circle/open star symbols). The simulated clumps are identified in mock Hα maps smoothed with a Gaussian aperture of 1 kpc, comparable to the typical resolution of the observed field galaxies.

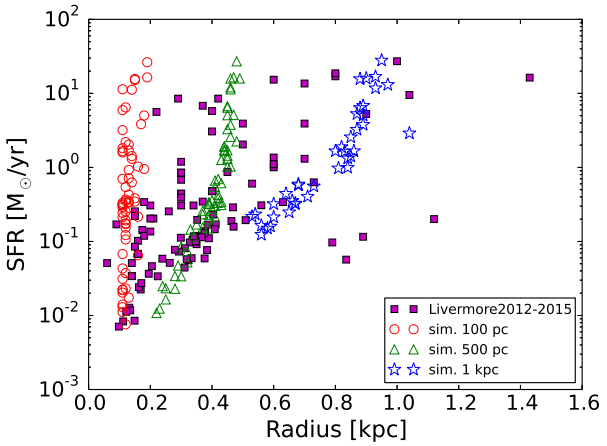

Figure 6. The comparison between clump SFR and radius distributions in simulations (empty symbols) and observations (filled squares). Observational data points are for lensed galaxies from Livermore et al. (2012, 2015), where the spatial resolution varies between 100 and 700 pc. The simulation results are shown for three different spatial resolution: 100 pc, 500 pc and 1 kpc, shown with red circles, green triangles and blue stars, respectively. The combination of simulations with different resolution and observations, which have a similar range of spatial resolution, matches very well. This suggests a correlation between clump radius and the spatial resolution used for observations.

galaxy and clumps identified in Hα since the former is sensitive to the bulk of stars while the latter closely trace the population of young stars and dense gas. In early stages of galaxy formation at high redshifts, both stellar and gaseous clumps should closely follow each other. To test this in our simulations, in Fig. 5 we show the mass versus radius distribution of Hα clumps in our simulations (empty circles) and compare it with the stellar mass contents of the same clumps (empty stars). Both the clump stellar and gas mass versus radius distributions are in good agreement with each other and in broad agreement with the observed stellar clump mass versus radius distribution.[5] To match this comparison as closely as possible to observational studies, we use our clump mass/size estimations after using a smoothing length of FWHM = 1 kpc, which is similar to the spatial resolution available to high-redshift observations (e.g. Förster Schreiber et al. 2011). We note, however, that the agreement between stellar and gaseous masses of our Hα clumps holds independent of the smoothing length.

In Fig. 6, we compare simulated clump SFR versus radius with observational data of lensed galaxies from Livermore et al. (2012, 2015),[6] after multiplying their reported SFRs by 1.7 required to make them consistent with the Salpeter initial mass function (Salpeter 1955) assumed in equation (2). Noting that the spatial resolution used for the observations (magenta squares) varies between 100 and 700 pc, we compare them with simulation results using three different spatial resolution: 100 pc, 500 pc and 1 kpc (red circles, green triangles and blue stars, respectively). The combination of simulations with different resolution and observations which have a similar range of spatial resolution matches very well. This suggests a correlation between clump radius and the spatial resolution used for observations.

[5] Due to differences in the method used for identifying stellar clumps compared to our Hα clumps, it is not sensible to directly compare our results with theirs. Therefore, we opted not to overplot the stellar clump mass versus radius distribution of Förster Schreiber et al. (2011) in Fig. 5.

[6] The galaxy stellar masses in the sample used by Livermore et al. (2012, 2015) is in the range 4×10^8–6×10^{10} M$_\odot$ while our galaxy stellar mass is 4×10^{10} M$_\odot$. We note, however, that we obtain very similar results using a simulation in which the stellar mass is ≈5 times lower. We found that reducing the stellar mass only results in fewer clumps in general without affecting their mass/radius distributions; see also Tamburello et al. (2015).

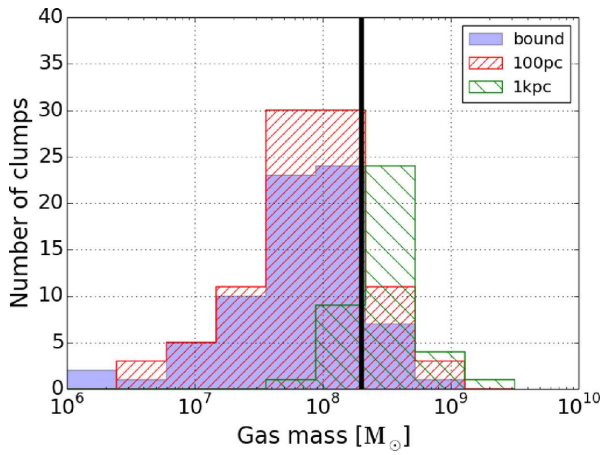

Figure 7. Comparison between the clump gas mass distribution using gravitationally bound structures in the simulation (filled histogram) and those found for the clumps in the Hα intensity maps using two different resolutions of 100 pc and 1 kpc (hatched histograms). The results are obtained by combining the simulation outputs at different times (i.e. 200, 300, 400 and 500 Myr). The black vertical line shows the Toomre mass estimated at the onset of the disc fragmentation, which coincidentally agrees well with the inflated clump mass distribution we found with the lower 1 kpc resolution.

Since in this paper we base our analysis only on Hα mocks, it is reasonable to ask how well the identification of clumps via Hα can capture the intrinsic properties of clumps, namely their radii and masses, when high resolution is available. This is important to address in order to conclude that the trends we have presented here are meaningful. A direct comparison between the clump gas mass estimated using bound structures in the simulation (using SKID group finder; see Tamburello et al. 2015) and those defined by identifying the clumps in the Hα intensity maps is shown in Fig. 7, where we combine the simulation results at different times (i.e. 200, 300, 400 and 500 Myr). The mass distribution of the

gravitationally bound clumps (filled histogram) is very similar to the mass distribution of H α clumps smoothed with 100 pc resolution (red hatched histogram). Using a lower resolution of 1 kpc for smoothing the H α maps results in a different distribution which peaks at a higher mass (green hatched histogram). Finally, the solid vertical black line in Fig. 7 indicates the Toomre mass calculated for our simulation (using $M_{\rm T} = \pi\Sigma \left(\frac{\lambda_{\rm T}}{2}\right)^2$, where $\lambda_{\rm T} = 2\frac{c_{\rm s}^2}{G\Sigma}$, and Σ and $c_{\rm s}$ are the gas surface density and the local sound speed, respectively) at the onset of disc fragmentation, using the local gas disc properties (see Tamburello et al. 2015). Interestingly, this agrees well with the inflated clump mass distribution we found with the lower 1 kpc resolution. However, this minimum Toomre mass estimation only has a small overlap with the high mass tail of the clump mass distribution using the higher 100 pc resolution. This highlights how using common notions and definitions of the fragmentation scale, taken from simple linear perturbation theory, can be extremely misleading, producing an apparent match with the data because of lack of resolution. This is not surprising as non-linear phenomena, such as disc fragmentation, are hardly described by linear theory, as discussed in detail elsewhere (Boley et al. 2010; Tamburello et al. 2015). The characteristic fragmentation mass in the simulation, which is recovered at higher spatial resolution, is much better matched with the modified Toomre mass proposed by Tamburello et al. (2015), which takes into account some of the non-linear aspects of the process.

4 SUMMARY AND DISCUSSION

Studying the nature of clumps observed in high-z galaxies has been subject to active theoretical work. However, there are some sensitive aspects which complicate the direct comparison between observations and model predictions. For instance, most theoretical studies use gas density distribution to identify clumps or interpret their properties, while observational studies are primarily based on detecting ionized gas and/or stellar emission, which does not necessarily trace the gas density. Moreover, the finite spatial resolution and sensitivity of observational studies should be taken into account when comparing with simulations which often have different resolutions. In this work, we tackled these two problems by post-processing hydrodynamical simulations of clumpy galaxies with accurate RT calculation which allows us to identify clumps in H α maps, similar to what is done in observational studies. In addition, we convolved the simulation outputs with different spatial resolutions in order to investigate the impact of resolution on the resulting clump properties.

We found that density peaks and peaks in H α emission do not always coincide with each other, mainly because H α emission is sensitive to both the gas density distribution and the distribution of young stars which are the main ionizing sources. The differences, however, are not large and the mass distribution of clumps found from H α maps is very similar to what one finds by identifying gravitationally bound objects considering only the gas density distribution (e.g. Tamburello et al. 2015). This shows that, provided that enough resolution and sensitivity are available, H α observations are a very powerful tool to study star-forming clumps and extract their physical properties in a meaningful way.

We found that the spatial resolution has a large impact on both mass and size of the clumps. Smoothing our simulate H α emission maps with Gaussians, with FWHM of 100 pc and 1 kpc, resulted in median clump masses 1.1×10^8 and 2.6×10^8 $M_\odot$, respectively. We found that the clump sizes are more sensitive to the spatial resolution where using smoothing lengths of 100 pc and 1 kpc resulted in median clump radii of 120 and 900 pc, respectively. Moreover, we found that varying the level of the error we added to our mock H α maps, namely 1, 5 and 10 per cent of the total luminosity, does not affect the distribution of clump sizes and/or masses.

In addition, we tested how the sensitivity (detection threshold) used for observing the clumps changes their observed properties. Changing the sensitivity by a factor of 10 (e.g. from SFR $>$ 1 to SFR $>$ 10 $M_\odot$ yr^{-1}) increases the typical clump stellar mass by nearly one order of magnitude. For a fixed detection threshold, however, changing the resolution from 100 pc to 1 kpc increases the typical clump stellar mass only by a factor of $\lesssim 2$. This result is nicely supported by the analysis of the measured clump stellar masses when data with different sensitivities and spatial resolutions are combined (Dessauges-Zavadsky et al. 2017).

The sensitivity of the clump properties to the spatial resolution and the detection threshold used to observe them has profound consequences for comparing models and observed data. For instance, as we showed in Tamburello et al. (2015), selecting clumps using the gas and stellar density distributions results in typical clump sizes in the range $\sim$100 pc, while high-z observations indicate typical clump sizes more than 10 times larger (e.g. Förster Schreiber et al. 2011). At first glance, this might indicate inconsistencies between model predictions and observations, but as we showed here, after convolving our simulated H α maps with a smoothing length similar to those typically accessible to high-z observations (i.e. $\gtrsim$1 kpc), we found clump sizes and masses very similar to those claimed by observational studies. This conclusion is in line with recent observations that used gravitational lenses to achieve a spatial resolution of $\sim$100 pc and found clumps much smaller than those typically found in high-z galaxies observed with $\sim$ kpc resolution (Jones et al. 2010; Livermore et al. 2012, 2015). These high-resolution observations found clump sizes very similar to what we found for our simulated H α maps using a smoothing length of 100 pc. This conclusion is also in good agreement with what Fisher et al. (2017) recently found for lower redshift disc galaxies with prominent substructures.

In this study, we used simulations which incorporate star formation and stellar feedback, and used detailed RT to calculate the H α properties of galaxies closely to what can be accessed in observations. The intrinsic properties of our clumps are in qualitative agreement with previous studies which did not include RT and/or star formation and stellar feedback (e.g. Ceverino et al. 2012; Behrendt et al. 2016). Moreover, we note that Behrendt et al. (2016) also found that a limited spatial resolution will lead to group together clumps smaller than the spatial resolution and infer inflated clump sizes.

Finally, it is important to note that the incorrect derivation of clump physical properties because of different observational limitations can lead to incorrect inferences on their nature, such as verifying that the observationally implied clump sizes match a fragmentation scale predicted by simple theoretical models that miss non-linear effects. This apparent match has provided major support to the notion that clumps are the products of disc fragmentation. As we have shown here, the match between the apparent typical clump mass and the Toomre mass in clumpy discs is primarily driven by the artificially inflated clump masses at low resolution and sensitivity (Fig. 7). Essentially, only the high mass tail of the clump mass distribution is comparable to the Toomre mass, which is rather an upper limit for the characteristic clump mass set by fragmentation in the non-linear regime, as explained in Tamburello et al. (2015). The characteristic mass is much better matched with the modified

Toomre mass proposed by Tamburello et al. (2015), while the tail of very massive clumps that lie even above the Toomre mass (see Fig. 7) results from later evolution, especially clump–clump mergers (Tamburello et al. 2015).

While we showed that the observed clump properties can be reproduced using simulations in which clumps are primarily formed through fragmentation processes, it does not imply that fragmentation is the only reasonable scenario for most of the observed star-forming clumps at high redshifts. Indeed, other processes such as minor mergers or accretion of the cores of disrupted satellites can also be plausible physical processes that lead to the formation of clumps, especially at the high mass tail of their distribution (Mandelker et al. 2017). If minor mergers are the dominant root for clump formation, their intrinsic size and masses are expected to be larger than what is expected from the disc fragmentation scenario, and one would expect the issues addressed in this paper to be less relevant and the intrinsically giant clumps remain large and massive even when increased resolution and sensitivity is achieved. The next generation of observations, especially those studying directly the gas phases with high resolution e.g. using the Atacama Large Millimeter Array (ALMA), should be able to uncover this alternative population of clumps.

We conclude that the discrepancies between clump properties found in observational studies, and between observations and simulations, can be significantly reduced by considering the different spatial resolutions accessible for the different studies, while still remaining in the context of the disc fragmentation scenario as the main origin for the clumps. While other important factors such as the specific nature of feedback can drastically change the intrinsic clump properties (Mayer et al. 2016), testing model predictions against observations requires to align them with the proper resolution and sensitivity.

ACKNOWLEDGEMENTS

This workis supported by the STARFORM Sinergia Project funded by the Swiss National Science Foundation. We thank the anonymous referee for his/her suggestions and comments which improved the manuscript.

REFERENCES

Adamo A., Östlin G., Bastian N., Zackrisson E., Livermore R. C., Guaita L., 2013, ApJ, 766, 105
Behrendt M., Burkert A., Schartmann M., 2016, ApJ, 819, L2
Behroozi P. S., Wechsler R. H., Conroy C., 2013, ApJ, 770, 57
Boley A. C., Hayfield T., Mayer L., Durisen R. H., 2010, Icarus, 207, 509
Bournaud F., 2016, in Astrophysics and Space Science Library, Vol. 418, Galactic Bulges. Springer International Publishing, Switzerland, p.355
Bournaud F., Elmegreen B. G., Teyssier R., Block D. L., Puerari I., 2010, MNRAS, 409, 1088
Ceverino D., Dekel A., Bournaud F., 2010, MNRAS, 404, 2151
Ceverino D., Dekel A., Mandelker N., Bournaud F., Burkert A., Genzel R., Primack J., 2012, MNRAS, 420, 3490
Dekel A., Krumholz M. R., 2013, MNRAS, 432, 455
Dessauges-Zavadsky M., Schaerer D., Cava A., Mayer L., Tamburello V., 2017, ApJ, 836, L22
Elmegreen D. M., Elmegreen B. G., Rubin D. S., Schaffer M. A., 2005, ApJ, 631, 85
Fisher D. B. et al., 2017, ApJ, 839, L5
Förster Schreiber N. M. et al., 2011, ApJ, 739, 45
Genzel R. et al., 2011, ApJ, 733, 101
Jones T. A., Swinbank A. M., Ellis R. S., Richard J., Stark D. P., 2010, MNRAS, 404, 1247
Kennicutt R. C., Jr, 1998, ApJ, 498, 541
Leitherer C. et al., 1999, ApJS, 123, 3
Livermore R. C. et al., 2012, MNRAS, 427, 688
Livermore R. C. et al., 2015, MNRAS, 450, 1812
Mandelker N., Dekel A., Ceverino D., DeGraf C., Guo Y., Primack J., 2017, MNRAS, 464, 635
Mayer L., Tamburello V., Lupi A., Keller B., Wadsley J., Madau P., 2016, ApJ, 830, L13
Moody C. E., Romanowsky A. J., Cox T. J., Novak G. S., Primack J. R., 2014, MNRAS, 444, 1475
Oklopcic A., Hopkins P. F., Feldmann R., Keres D., Faucher-Giguere C.-A., Murray N., 2017, MNRAS, 465, 952
Osterbrock D. E., Ferland G. J., 2006, Astrophysics of gaseous nebulae and active galactic nuclei, 2nd ed. University Science Books, Mill Valley, CA
Pawlik A. H., Schaye J., 2008, MNRAS, 389, 651
Pawlik A. H., Schaye J., 2011, MNRAS, 412, 1943
Rahmati A., Pawlik A. H., Raicevic M., Schaye J., 2013a, MNRAS, 430, 2427
Rahmati A., Schaye J., Pawlik A. H., Raicevic M., 2013b, MNRAS, 431, 2261
Salpeter E. E., 1955, ApJ, 121, 161
Stinson G., Seth A., Katz N., Wadsley J., Governato F., Quinn T., 2006, MNRAS, 373, 1074
Swinbank A. M., Smail I., Sobral D., Theuns T., Best P. N., Geach J. E., 2012, ApJ, 760, 130
Tacconi L. J. et al., 2010, Nature, 463, 781
Tamburello V., Mayer L., Shen S., Wadsley J., 2015, MNRAS, 453, 2490
Wisnioski E., Glazebrook K., Blake C., Poole G. B., Green A. W., Wyder T., Martin C., 2012, MNRAS, 422, 3339

This paper has been typeset from a TEX/LATEX file prepared by the author.